

Applied Acoustics

Acoustic detection and localisation system for *Hylotrupes bajulus* L. larvae using a MEMS microphone array --Manuscript Draft--

Manuscript Number:	APAC-D-23-00403R3
Article Type:	Research Paper
Section/Category:	Europe and Rest of the World
Keywords:	Wood-boring larvae identification; Beamforming; MEMS microphone array; Timber trade safeguard; Targeted treatment methods
Corresponding Author:	Lara del Val University of Valladolid SPAIN
First Author:	Roberto Diego Martinez, Ph.D.
Order of Authors:	Roberto Diego Martinez, Ph.D. Alberto Izquierdo, Ph.D. Juan José Villacorta, Ph.D. Lara del Val, Ph.D. Luis-Alfonso Basterra, Ph.D.
Abstract:	<p>A novel system for acoustic detection of the presence of xylophagous insect larvae inside structural timber beams is presented. It is based on an extensive array of MEMS microphones that allows the acoustic detection and localisation of the larvae when they are active. In a first phase, the activity of the larvae is continuously detected by means of frequency filtering and a sliding energy estimator, and after that, a set of short-duration segmented signals is generated, which obtains the spatial localisation of the larvae, by means of a shaping algorithm based on delay-sum beamforming techniques. The tests carried out demonstrate that it is possible to detect and locate multiple larvae of <i>Hylotrupes bajulus</i> L. inside structural-sized pieces of wood of <i>Pinus sylvestris</i> L., as well as their internal trajectory.</p> <p>In the future, the system could address the identification of the specific type of xylophage responsible for the deterioration by using machine learning or equivalent techniques, based on the temporal and frequency information of the detected sound events.</p> <p>The aim of this work is to control unintentional infections in the international timber trade, in the assembly and the use of infected timber and, in all cases, to be able to carry out selective, targeted and localised treatments and to verify their success.</p>
Suggested Reviewers:	Ignacio Segundo Bobadilla, Dr. Professor, Polytechnic University of Madrid i.bobadilla@upm.es Francisco Arriaga, Dr. Full Professor, Polytechnical University of Madrid f.arriaga@upm.es Romina María del Rey Tormos, Dr. Professor, Universidad Politécnica de Valencia roderey@fis.upv.es
Opposed Reviewers:	
Response to Reviewers:	

Dear Reviewers,

We express our sincere appreciation for your decision and the valuable insights and thoughtful critique you have provided on our manuscript. As we mentioned previously, your in-depth reviews have been integral in refining our work and enhancing its quality.

As requested, we have outlined the modifications made to the manuscript. For ease of reference, we have highlighted these changes in the manuscript using a yellow colour.

Once again, thank you for your valuable contribution to this research endeavour.

Best Regards,

Lara del Val

Modifications made to the manuscript in response to reviewers' questions

- Page 15

Lines 394-395: The final sentence is: "*The study could also be extended to the detection of the feeding patterns and the galleries of other xylophagous organisms, such as common woodworm or termites.*".

Highlights

- A non-contact low-cost acoustic system allows the detection and localisation of cerambycid larvae when they tear wood to feed.
- Acoustic system based on a low-cost MEMS microphone array.
- The presented system can be used to carry out specific wood treatments as opposed to the extensive treatments currently used.
- The study could also be extended to the detection of other xylophages, such as common woodworm or termites.

Acoustic detection and localisation system for *Hylotrupes Bajulus* L. larvae using a MEMS microphone array

Roberto D. Martínez¹, Alberto Izquierdo², Juan José Villacorta², Lara del Val^{2*}, Luis-Alfonso Basterra³

¹Department of Agricultural and Forestry Engineering. E.T.S.I Agrarias. University of Valladolid (Spain). Avenida de Madrid, 57. - 34004, Palencia (Spain).

²Department of Signal Theory and Communications and Telematic Engineering. ETSI Telecomunicación. University of Valladolid (Spain). Paseo Belén, 15.- 47011 Valladolid (Spain)

³Timber Structures and Wood Technology Research Group. ETS Arquitectura. University of Valladolid (Spain). Avenida de Salamanca, 18.- 47014 Valladolid (Spain)

*Author to whom correspondence should be addresses: lara.val@uva.es

Abstract

A novel system for acoustic detection of the presence of xylophagous insect larvae inside structural timber beams is presented. It is based on an extensive array of MEMS microphones that allows the acoustic detection and localisation of the larvae when they are active. In a first phase, the activity of the larvae is continuously detected by means of frequency filtering and a sliding energy estimator, and after that, a set of short-duration segmented signals is generated, which obtains the spatial localisation of the larvae, by means of a shaping algorithm based on delay-sum beamforming techniques.

The tests carried out demonstrate that it is possible to detect and locate multiple larvae of *Hylotrupes Bajulus* L. inside structural-sized pieces of wood of *Pinus sylvestris* L., as well as their internal trajectory.

In the future, the system could address the identification of the specific type of xylophage responsible for the deterioration by using machine learning or equivalent techniques, based on the temporal and frequency information of the detected sound events.

The aim of this work is to control unintentional infestations in the international timber trade, in the assembly and the use of infested timber and, in all cases, to be able to carry out selective, targeted and localised treatments and to verify their success.

Introduction

The degradation of structural timber by attacks of xylophagous insects is a global problem that is partly unavoidable as wood is sensitive to the laws of survival inherent to the nature from which it originates. Under certain conditions, the risk of attack by decay fungi and different kinds of insects can be high. Preventive and curative treatments, once the attack has already occurred, cause enormous economic costs worldwide.

Hylotrupes Bajulus L. (house longhorn beetle) is a species of European origin that has spread throughout most of the world (Vives 2000). Its larvae are polyphagous and can live and feed on many types of wood with low moisture content, where they can remain for several years until they reach the development necessary to pupate. They generally live in coniferous woods of genera such as *Pinus*, *Abies* and *Picea*, although they have also been reported on *Populus*, *Quercus*, *Acacia*, *Salix*, etc. (Vives 2000). Due to its ability to attack almost any type of wood and its resistance, it is the cerambycid that can cause the greatest damage to structural wood, carpentry and furniture and has been extensively studied in most treatises on insect pests (Demelt

1966; Zarco 1935; Ruiz 1942; Duffy 1957; 1953). Its larvae lodge inside the wood, usually at a shallow depth, and move very slowly. For this reason, visual inspection systems have traditionally been used to detect them, based on the location and identification of the detritus and the exit holes of the adult insect; careful listening to the sound made by its specimens when biting the wood, which requires considerable expertise and is subject to subjectivity and the influence of background noise; and others based on more or less complex instrumentation.

Acoustic emissions (AE) are elastic waves in solid materials caused by fractures in macro- or microstructures or by friction, used routinely as a standard method to study fatigue and other phenomena in materials engineering. In wood, the possibility of recording sounds or recording AE with the aim of identifying active insect attack has long been published (Pence et al. 1954; Pallaske 1986) (Fujii et al. 1989) and in recent years has received renewed attention (Nowakowska et al. 2017) incorporating signal analysis and artificial intelligence (Bilski et al. 2016). Plinke (2021) have published recent advances in the measurement and evaluation of emitted acoustic signals, with some limitations regarding the placement of the sensors, which must be in firm contact with the wood, and the temporary inactivity of the larvae. Commercial "remote sensing" applications are also becoming available (Potamitis et al. 2019). Current methods focus on detection, but do not provide information on larvae location. In contrast, there are numerous works on acoustic geolocation of terrestrial higher animals such as elephants, wolves and marine animals such as whales (Dissanayake et al. 2018a; Noad, et al. 2004; Kershenbaum et al. 2019; Dissanayake et al. 2018b). The aim of this work has been to find and develop a low-cost, non-contact technique, using a MEMS microphone array, capable of detecting and accurately locating active house longhorn beetle larvae inside wood. The system is aimed at controlling infections in museums and other places where the protection of heritage wood is needed, unintentional infections in the international timber trade, in the assembly and use of infected wood, and, in all cases, it allows for the execution of selective, targeted and localized treatments and the verification of their success.

2. Description of the acquisition system (AIF)

The acquisition system used consists of 3 elements: 1) an acoustic array of MEMS microphones; 2) an acquisition and pre-processing system based on FPGA/Processor and 3) a PC-based analysis, detection and visualisation application. All software developed on the different platforms is original and has been done using the LabVIEW 2021 programming language. A block diagram of this acquisition and pre-processing system is shown in Figure 1.

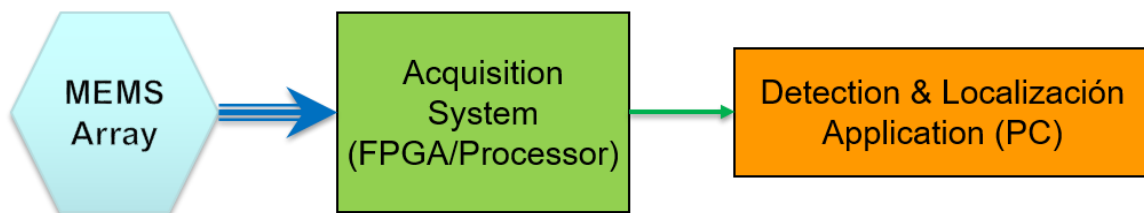


Figure 1. Block diagram of the acquisition and pre-processing system.

2.1 Acoustic Array

An array is an arranged set of identical sensors working in a coordinated manner (Van Trees 2002). In this case, microphone arrays, working together with beamforming techniques (Van Veen and Buckley 1988), allow the localisation of acoustic sources (Tiete et al. 2014; Edstrand et al. 2011; Zhang et al. 2014).

90 The acoustic array used in this work consists of digital MEMS microphones. The acronym MEMS
 91 (Micro-Electro-Mechanical Systems) refers to mechanical systems with a dimension of less than
 92 1 mm (Hsieh et al. 2002) in the field of integrated circuits (ICs). In the case of MEMS
 93 microphones, each of the chips that make them up includes a microphone, a signal conditioner
 94 and an acquisition device (Beeby et al. 2004). These characteristics of these sensors make it
 95 possible to have acoustic arrays with a large number of channels, at a reduced cost and size.

97 *2.1.1 Nearfield beamforming*

98 Assuming a plane wave $x(t)$ with a direction of arrival θ , and a linear array with N sensors
 99 separated a distance d , the signal received at each sensor x_n , is a phase-shifted replica of $x(t)$. A
 100 beamformer combines linearly the signals x_n , which are previously multiplied by complex weights
 101 w_n , obtaining an output signal $y(t)$. Figure 2, shows the general structure of a beamformer.

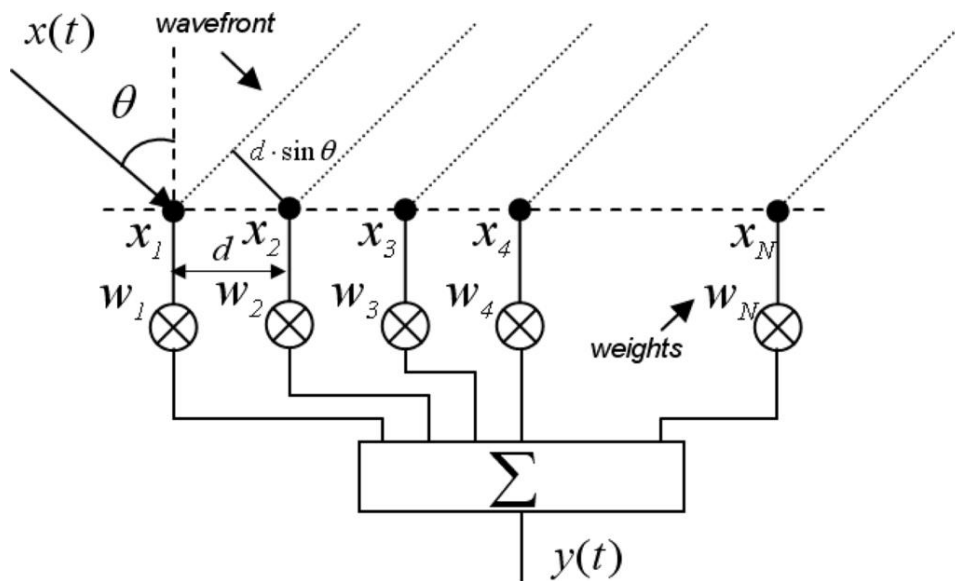


Figure 2. Structure of a beamformer.

105 Using the appropriate weights allows spatial filtering, giving greater gain to signals arriving from
 106 a given direction, called steering angle, over the rest. (Naidu 2001; Van Veen and Buckley 1988).
 107 The graphical representation of the spatial response of a beamformer versus the angle or the
 108 direction of arrival is called the beampattern. It should be noted that the beampattern is also highly
 109 dependent on the position of the sensors within the array, known as array geometry.

110 Beamformers can be classified as data independent or as statistically optimum, depending on the
 111 weights selection (Van Veen and Buckley 1988). The weights in a data independent beamformer,
 112 which has been used in this work, do not depend on the array data and are chosen to show a
 113 specified response for all working scenarios. The simplest data-independent beamformer is the
 114 Delay-and-Sum beamformer (Brandstein and Ward 2001), which applies time delays to the
 115 signals obtained by the array sensors to compensate for delays in the arrival of the signal of
 116 interest at each array sensor due to the signal propagation itself. In this way, the signals are aligned
 117 in time and subsequently summed, forming a single output signal $y(t)$, as shown in Figure 3. The
 118 Delay-and-Sum beamformer corresponds, for the general beamformer shown in Figure 2, to the
 119 specific case of using w_n weights of amplitude 1 and phases equivalent to the delays associated
 120 with each of the sensors.

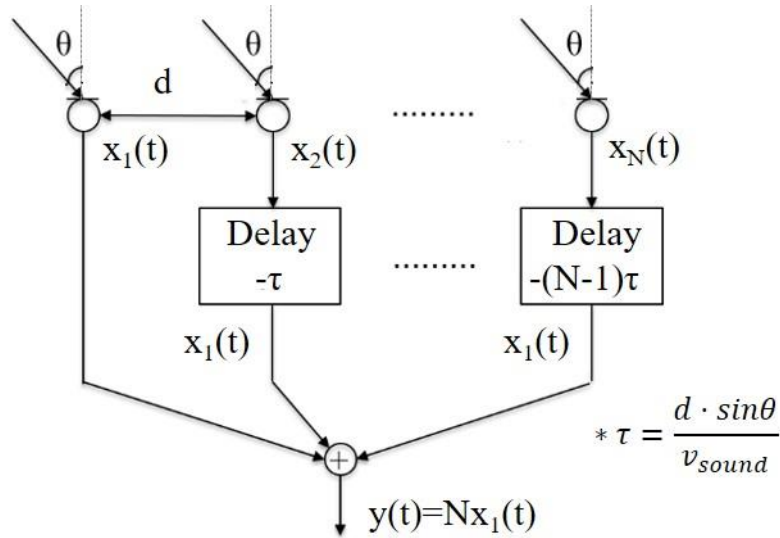


Figure 3. Delay and Sum beamformer.

The classical delay and sum beamformer is based on the consideration that the source of the signal to be detected is far enough away from the array to assume a far-field situation, so that the delay with which the signal reaches each sensor in the array depends only on the position of the sensor and the pointing angle. Despite this fact, it should be noted that in the system presented in this study these far-field conditions are not met, but it is possible to use the considerations of the delay and sum conformer in near-field conditions (Kennedy et al. 1998, Cho and Roan 2009, He et al. 2012), as is the case. In near-field conditions, what must be taken into consideration is that the associated time delays also depend on the relative distance from the emitter to each sensor in the array, as a spherical propagation of the signal must be assumed, as can be observed in Figure 4.

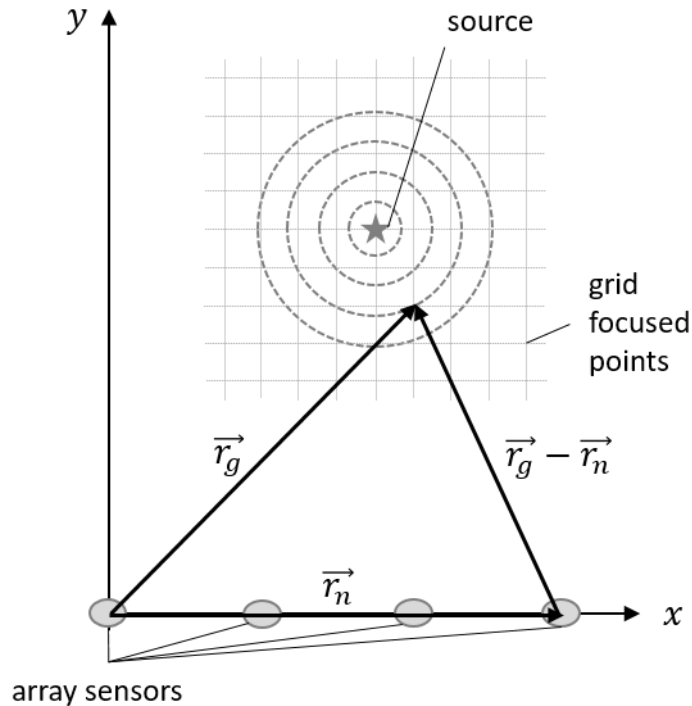


Figure 4. Nearfield considerations.

135 Since in this case the plane where the sounds (the larvae emissions) are originated is known, the
 136 exact delay associated to the propagation of the signal between each of the grid points defined in
 137 the analysis/emission plane and each sensor of the array can be determined and used in the delay
 138 and sum algorithm. So, the array output in this case can be expressed by

$$139 \quad y(\vec{r}_g, t) = \frac{1}{M} \sum_{n=1}^N w_n \cdot x_n(t - \tau_n(\vec{r}_g))$$

140 where \vec{r}_g represents the distance of the reference point to one of the focused points defined by the
 141 grid. The reference point is arbitrarily defined. In the specific case shown in Figure 4, is the first
 142 sensor on the left of the array. As it was indicated in Figure 2, N is the number of the sensors, w_n
 143 is the weight applied to the n channel of the array (which is equal to 1, as a delay and sum
 144 beamformer has been used), and $x_n(t)$ represents the signal acquired by sensor n of the array.
 145 $\tau_n(\vec{r}_g)$ indicates the individual time delay of sensor n of the array to the reference point,
 146 considering that the signal is a spherical wave, and it is obtained by

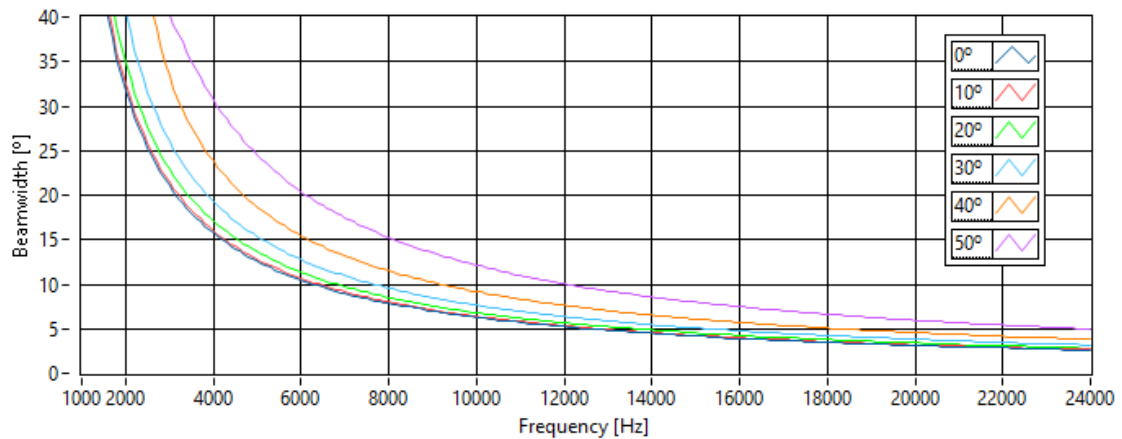
$$147 \quad \tau_n(\vec{r}_g) = \frac{|\vec{r}_g| - |\vec{r}_g - \vec{r}_n|}{v_{sound}}$$

148 where \vec{r}_n represents the distances of the reference point to sensor n of the array.

150 2.1.2 Array performance

151 In this study, a planar array has been used, with its elements distributed on a completely flat
 152 surface. In the case of a linear array, one direction of arrival can be discriminated, whereas using
 153 a two-dimensional, or planar, array two-dimensional information on the location of acoustic
 154 sources, which in this case are none other than the larvae, can be obtained, as the corresponding
 155 array response is a 2D beampattern. Specifically, this array consists of 486 SPH0641LU4H-1
 156 digital MEMS microphones of Knowles (“SPH0641LU4H-1 MEMS Microphone” n.d.), and has
 157 a spatial aperture of about 35 cm, in both spatial dimensions.

158 The angular resolution of the 2D array used depends basically on the working frequency and the
 159 pointing angle, as shown in Figure 5. In this figure it can be observed that the beamwidth
 160 decreases as the analysis frequency of the acoustic emissions increases. It can also be noted that
 161 the beamwidth widens as the pointing angle increases from the boresight, i.e., pointing at 0° , to
 162 the maximum pointing excursion of 50° defined for this study. The smaller the beamwidth the
 163 better the angular resolution and the more accurately the position of the larvae on the beams under
 164 test, as well as the position of two larvae in close proximity, can be determined.



165

Figure 5. Array beamwidth vs. Working frequency and pointing angle

Establishing a maximum angular resolution of 10° , and a maximum angular excursion of 50° for the acoustic beams, it can be inferred that the minimum working frequency must be higher than 12 kHz. Specifically, working in the 12 kHz to 24 kHz frequency band, the beamwidths vary between 2.6° and 10° . For practical purposes, the frequency band of interest has been reduced to the range between 13 kHz and 23 kHz to allow proper implementation of the necessary digital bandpass filters.

In previous works reviewed, related to roundheaded wood borer larvae (Mankin 2008, Mankin 2011, Sutin 2019, Mankin 2021), the corresponding acoustic emissions were characterized in bands with maximum frequencies of 10 kHz, typically using piezoelectric sensors and accelerometers in contact with the piece of wood under analysis. But there are also works (Mankin 2011, Sutin 2019) that describe the usefulness of the ultrasonic band. Therefore, the use of this new working frequency band allows exploring its potential for detection and for localization using acoustic arrays. Specifically, the chosen working band: i) takes advantage of the frequency response of MEMS microphones that have a high sensitivity to high frequencies (“SPH0641LU4H-1 MEMS Microphone” n.d.), and ii) reduces the contribution of ambient noise by discarding low frequencies (Mankin 2011).

2.2 Acquisition and processing system

The base unit of the acquisition system is an sbRIO 9607 platform (“SbRIO-9607 Platform” n.d.). This platform belongs to National Instruments, particularly to the Reconfigurable Input-Output (RIO) family of devices. Specifically, this sbRIO platform is an embedded single-board controller, running NI Linux Real-Time with an FPGA Zynq-7020 and a dual-Core 667MHz processor. The FPGA has 96 digital inputs/outputs, of which 81 are used as the connection interface with 162 MEMS microphones of the array, so that in each I/O line, two microphones are multiplexed, while the other lines are used to generate the clock and synchronise. The processor is equipped with 512 MB of DDR3 RAM, 512 MB of built-in storage space, USB Host port, and Giga Ethernet port. Specifically, 3 interconnected cards have been used to guarantee the synchronous capture of the 486 sensors of the used array.

2.3 Analysis, localisation and visualisation software

Based on a Personal Computer and in LabVIEW 2021 programming language, specific software has been developed that handles the following tasks:

- Control of the capture operations of the 3 acquisition cards in a synchronised manner.
- Detection of larvae activity on a continuous basis.
- Storage of the detected signals for further segmentation to isolate the short duration sounds (typically 1-2 ms) produced by the larvae when biting wood.
- Implementation of beamforming algorithms to localise the position of the detected sounds.
- Finally, implementation of a control interface to display a 2D image with the localised positions over an established time frame.

209 **3. Test setup**

210 This section describes the setup of the measurement system inside an anechoic chamber which is
211 based on an extensive array of MEMS microphones. It also describes the setup of the wooden
212 beams and how 6 larvae have been implanted. Finally, a temporal and frequency characterisation
213 of the captured signals is given.

214 **3.1 Test set-up**

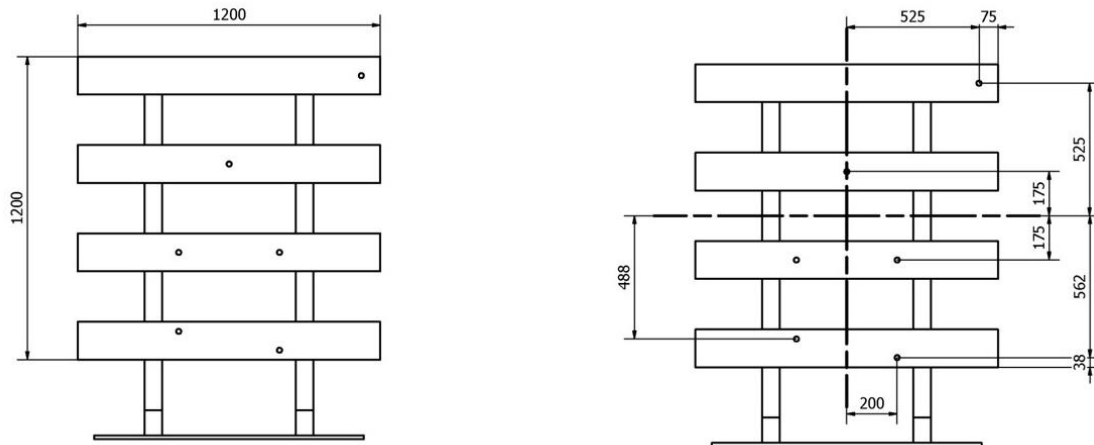
215 6 larvae of *Hylotrupes bajulus* L. weighing between 0.22 g and 0.35 g were implanted in 4 pieces
216 of wood measuring 90x140x1200 mm of Scots pine (*Pinus sylvestris* L.), previously conditioned
217 to a moisture content of 12%. The larvae were extracted from demolished wood from historical
218 buildings in the city of Valladolid, Spain.

219 To implant the larvae, a hole was made in the opposite side of each piece of wood, so that the end
220 of the hole was 10 mm from the sapwood observation side. The larva is placed at the end of the
221 hole and the hole is sealed with tissue paper. The larvae are distributed in such a way that different
222 phenomena of sound propagation in wood, edge effect, etc. can be studied.

223 Once the larvae have been implanted in the wooden specimens, the initial position of the larvae
224 is marked on the corresponding wooden parts with a yellow sticker, and the wooden specimens
225 are placed in a frame to facilitate their simultaneous study (Figure 6). This set-up makes it possible
226 to simulate the presence of several simultaneous infestations. The larvae are allowed to
227 acclimatise for 30 days. After this time the listening tests are started.

228 The test setup is implemented inside an anechoic chamber, placing the listening system, i.e., the
229 MEMS microphone array, parallel to the frame, centred with respect to the wooden parts, and 600
230 mm apart (Figure 7). The environmental conditions in the anechoic chamber were approximately
231 24°C and 40 % RH. Figure 8 shows an image of the set-up implemented for the tests.

232 To check the final location of the larvae, a manual milling machine was used to remove the larvae.



233

234 Figure 6. Location of the 6 larvae within the wooden frame. Distances in mm.

235

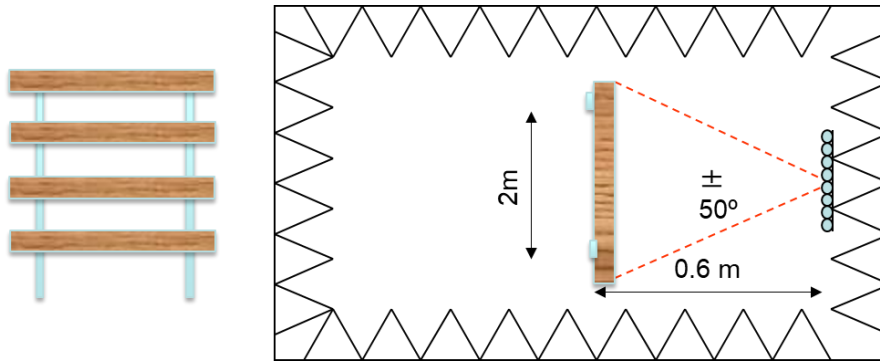


Figure 7. Test set-up inside the anechoic chamber.

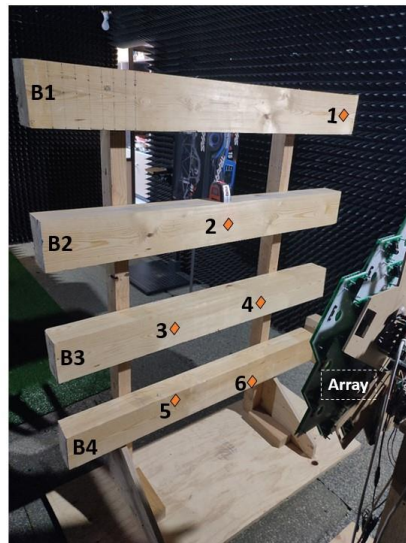


Figure 8. Image of the setup used. B#: beam. n°: Initial position of larva n.

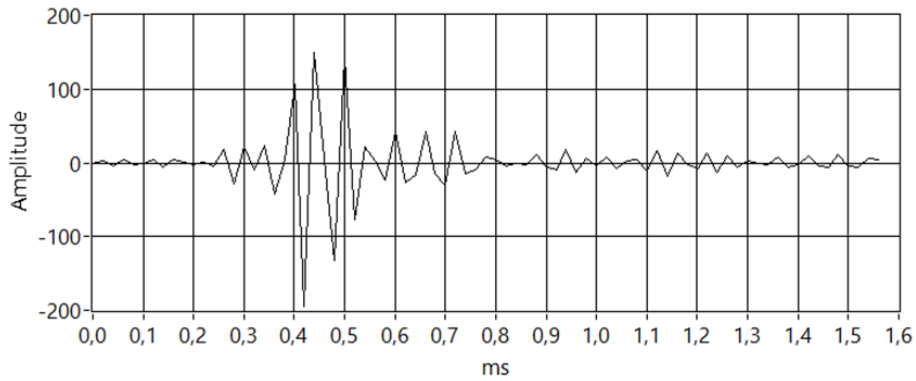
3.2 Time and frequency characterisation

Based on the signals analysed during the acquisition phase, where more than 50000 detections generated by the 6 larvae were obtained, their duration and spectrum were characterised. Traditionally, acoustic detection systems work in the band between 80 Hz and 8000 Hz (R. Mankin et al. 2021) and can even go up to 10 kHz (R. W. Mankin et al. 2008; n.d.) due to the limited bandwidth of the accelerometers used and the low sensitivity of microphones at higher frequencies.

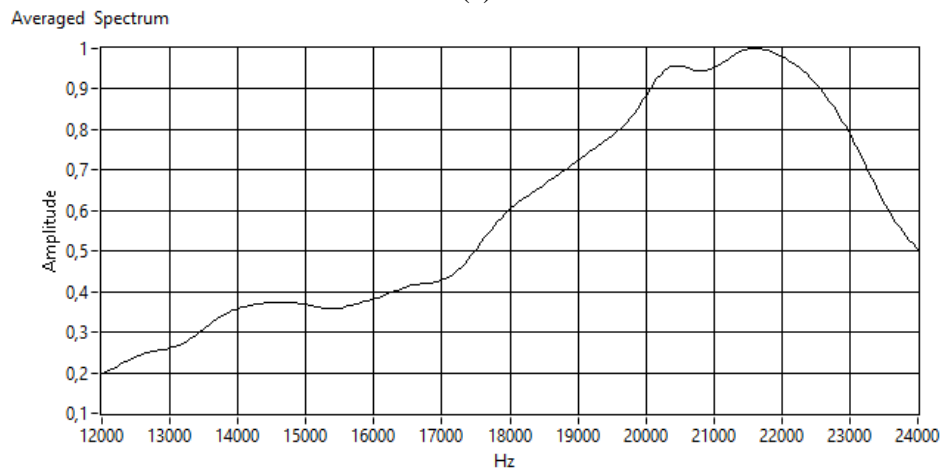
In the acquisition system used, based on an array of MEMS microphones, it must be considered that the overall sensitivity of the system is very high due to having hundreds of microphones working together and that the angular resolution, which is necessary to locate the position of the larvae accurately, improves as the working frequency gets higher.

The array used allows angular resolutions of between 4° and 8° depending on the working frequencies. On the other hand, this array has a gain of 26 dB, which allows the remote detection and localisation of very weak acoustic signals, such as those generated by *Hylotrupes bajulus* L. larvae.

257 The signals emitted by the larvae have a typical duration of 1 ms. Figure 9a shows a time-lapse
258 realisation of one of these captures. On the other hand, Figure 9b shows the corresponding average
259 spectrum of the emitted signals in the defined working frequency band. Based on this information,
260 a band-pass filter will be applied to the signals and a segmentation will be performed as detailed
261 in later sections.



(a)



(b)

262 Figure 9. a) Captured filtered time signal. b) Averaged spectrum.

263

264 4. Processing algorithm

265 As functionally described, the implemented processing algorithm consists of the chain of sub-
266 algorithms illustrated in Figure 10 and described below.

267

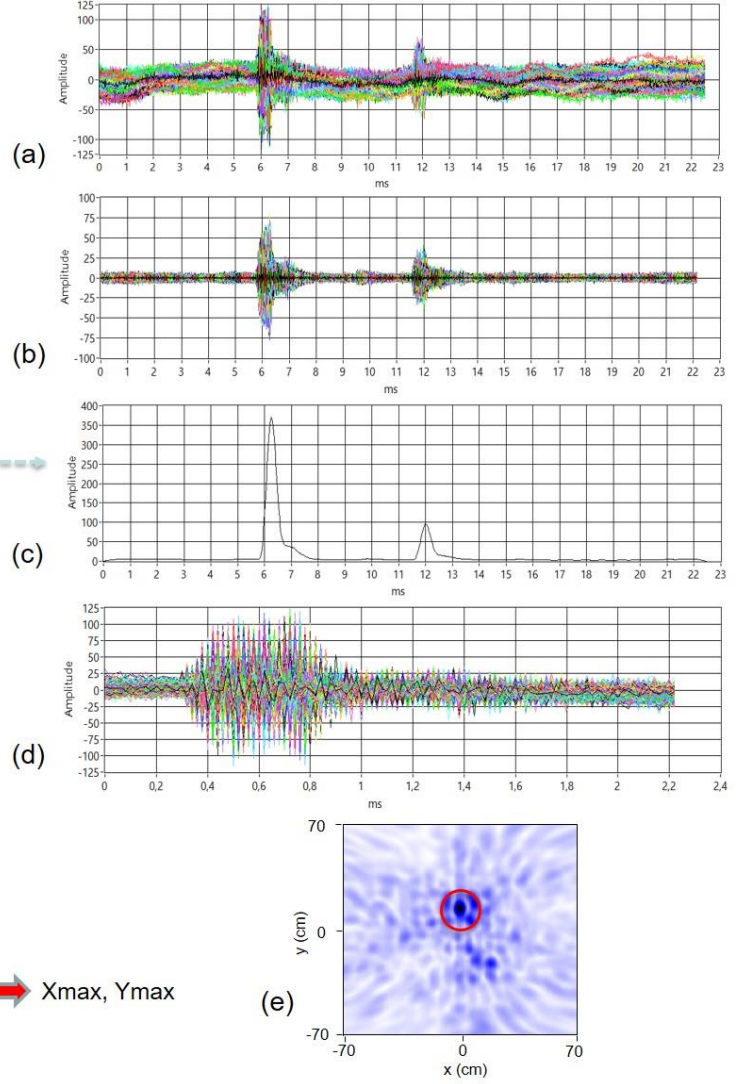
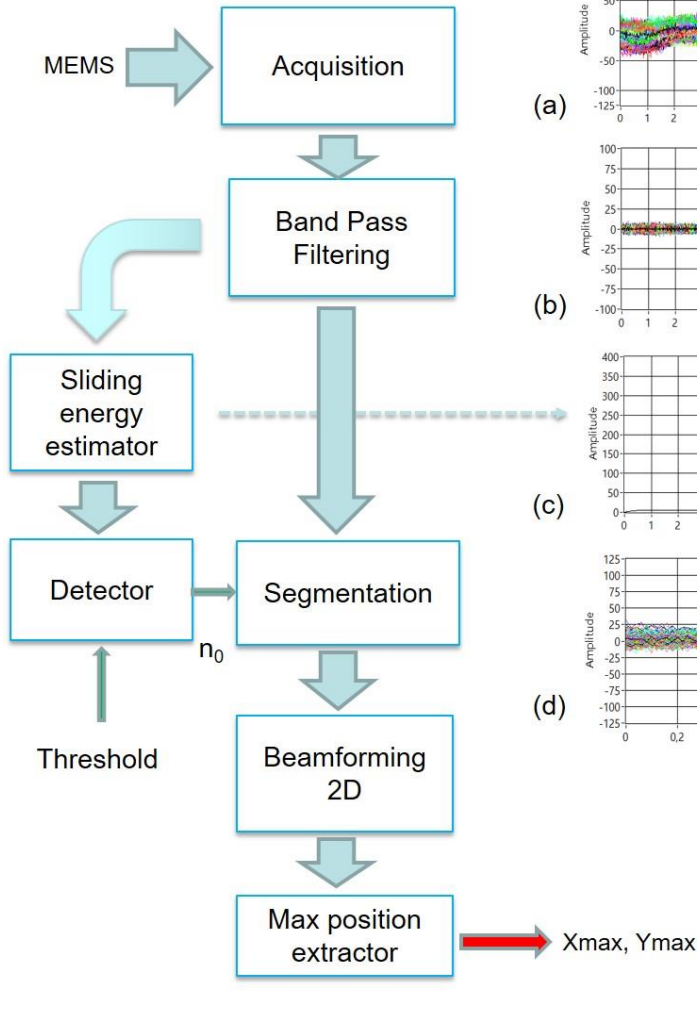


Figure 10. Processing steps and corresponding signals.

The acquisition system operates continuously, capturing N samples of a signal x_k of 22.5 ms duration with a sampling frequency f_s of 50 kHz, for each of the K sensors that make up the array. A digital anti-aliasing filter with an equivalent cut-off frequency of 24.5 kHz has been included. An example of the K acquired signals can be observed in Figure 10a.

$$x_k[n] = x_k(nT), \quad T = 1/f_s, \quad n = 0 \dots N - 1, \quad k = 0 \dots K - 1$$

First, each of the captured signals is filtered by a digital bandpass FIR filter ($h[n]$), with a passband between 13 kHz and 23 kHz, with a transition band of 500 Hz, designed from the window technique, making use of a Hamming window. The K filtered signals of the example are shown in Figure 10b.

$$y_k[n] = x_k[n] * h[n]$$

The next step is to detect whether there is activity of any of the larvae in the captured signal. To do this, the sliding energy $E_k[n]$ is calculated over a window of 2 ms for each of the filtered signals using the localised energy technique. The average of the energy estimators $E_k[n]$ is then calculated, as shown in Figure 10c.

$$E_k[n] = \sum_{r=0}^{N-1} y_k[r]^2 \cdot w[r-n]^2, \quad w[n] = 1 \quad 0 \leq n \leq M-1, \quad M = \frac{2 \cdot 10^{-3} s}{T}$$

$$E_{mean}[n] = mean\{E_k[n]\}$$

The estimator $E_{mean}[n]$, is compared with a threshold and in case it exceeds it, the position of the first maximum of the energy n_0 is searched for a segmentation. The threshold value is selected so that the system does not detect ambient noise in the test room. In the tests it is assumed that only one larva is active. If there were several active larvae during the 25 ms captures, E_{mean} would show several maxima. In this case, it would be necessary to select only one of the maxima for the subsequent shaping algorithm to correctly identify the position of a larva.

$$n_0 = \min\{n\} \mid E[n] \geq threshold$$

In the segmentation, for each of the 25 ms $y_k[n]$ filtered signals, a segment of 2 ms duration is extracted, indexed by n_0 , so that it contains the acoustic signal emitted by the larva. The corresponding segmented signals are shown in Figure 10d.

$$z_k[n] = y_k[n - n_0] \cdot w[n], \quad w[n] = 1 \quad 0 \leq n \leq M-1, \quad M = \frac{2 \cdot 10^{-3} s}{T}$$

Using beamforming techniques, and specifically the Delay and Sum algorithm adapted to nearfield conditions, an acoustic image is constructed from the generation of $L_1 \times L_2$ shaped beams to analyse the corresponding spatial positions in the plane containing the 4 wooden beams under analysis. The plane to be analysed, which is the one where the larvae are, is divided into L_1 positions in the horizontal coordinate and L_2 positions in the vertical coordinate, and each of the shaped beam points to each of the $L_1 \times L_2$ intersections, as shown in Figure 11. In the experiment carried out, this plane has dimensions of 120 x 120 cm, and is analysed with a resolution of 2 cm in both coordinates, so that a total of 61x61 beams were generated.

$$B_{i,j}[n] = Delay\&Sum\{z_k[n]\}, \quad 0 \leq i \leq L_1 - 1, \quad 0 \leq j \leq L_2 - 1$$

Finally, the energy of the shaped beams is calculated and plotted, forming an acoustic image of the analysis plane containing the 4 wooden beams. The corresponding acoustic image of the example can be seen in Figure 10e.

$$E[i,j] = \sum_n (B_{i,j}[n])^2$$

From the acoustic image, the coordinates of the maximum of the image are obtained (X_{max} , Y_{max}), which would correspond to the position detected for the larva.

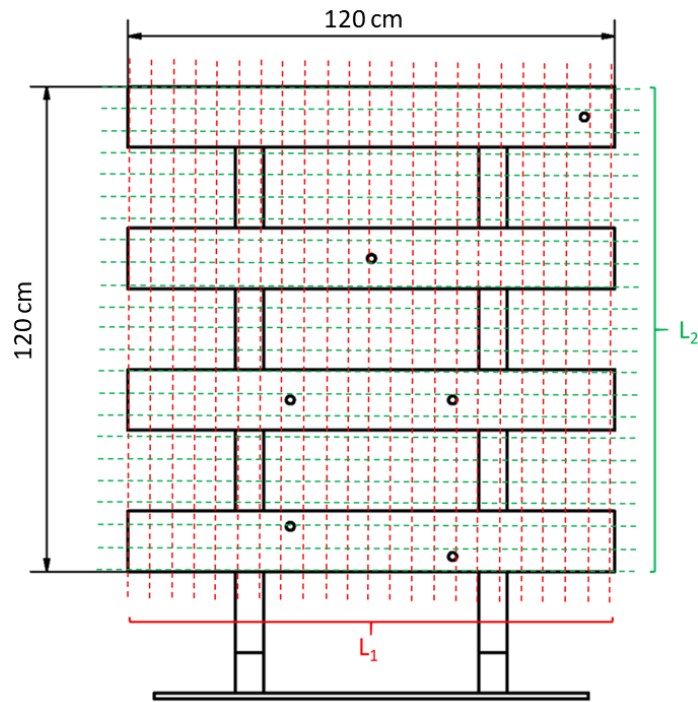


Figure 11. Assessment positions for beamforming.

5. Analysis of results

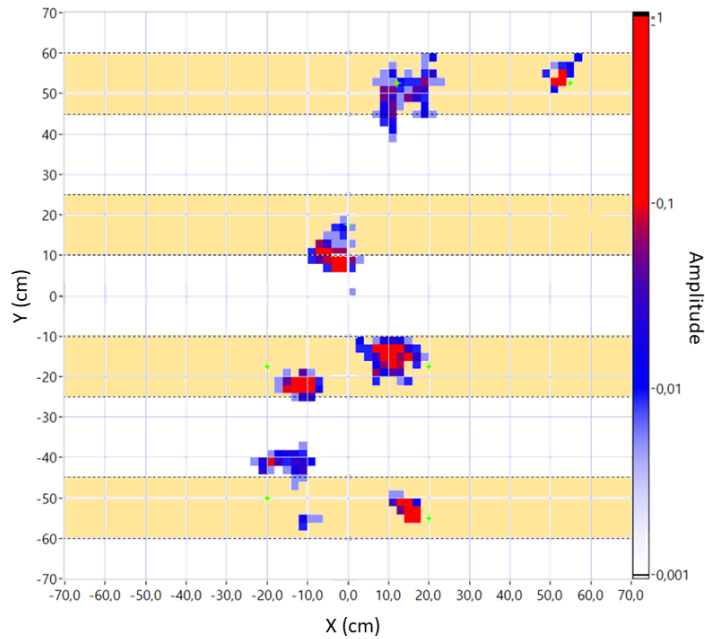
After acquiring about 2.5 million captures, over a period of 2 months, 50000 captures were obtained in which there was activity of the implanted larvae, which is 2% of the number of captures. In this section we will first analyse the acoustic images obtained based on the algorithm described in Section 4. Then we will verify the behaviour of the larvae and the extent of the galleries drilled during the analysis period.

5.1 Acoustic image analysis

For the analysis of the larvae positions, a 2D histogram has been made with the positions of the maximum of each of the 50000 acoustic images, as can be observed in Figure 12. In this 2D histogram, in addition, the initial positions of the 6 larvae have been marked with a green cross. The boundaries of each of the 4 wooden beams under analysis are also marked by brown dashed lines. To calculate the histogram, the number of times the position of the maximum (X_{max} , Y_{max}) fell into one of the 61x61 defined cells (Figure 11) was counted. The values have been normalised and fitted to a colour map on the Z-axis. There are 7 zones where the maximums of the acoustic images are concentrated, with variable dispersions for each of the larvae since the activity of each of them during the period of analysis and their movements have been variable.

At this point, it should be pointed out that the sound produced by each larva has complex propagation mechanisms, due to the fact that wood is not a homogeneous medium, and the larvae produce internal galleries, so that the sound is generated at one point and then comes out to the surface of the beam through another point, which is experimentally proven to be close to the internal position where it was generated. In addition, there are knots and cracks in the beams that can also alter the exit point of the sound. It is therefore clear that the sound exit points are close to the position where the larvae are located, but that if there are significant fibre deviations, knots or cracks in the beams, the sound will also exit through them. A visual inspection is required to

342 rule out a sound emission zone if there is a band or knot in its proximity and therefore that the
 343 remaining detected zones clearly identify the position of the larvae inside them.



344

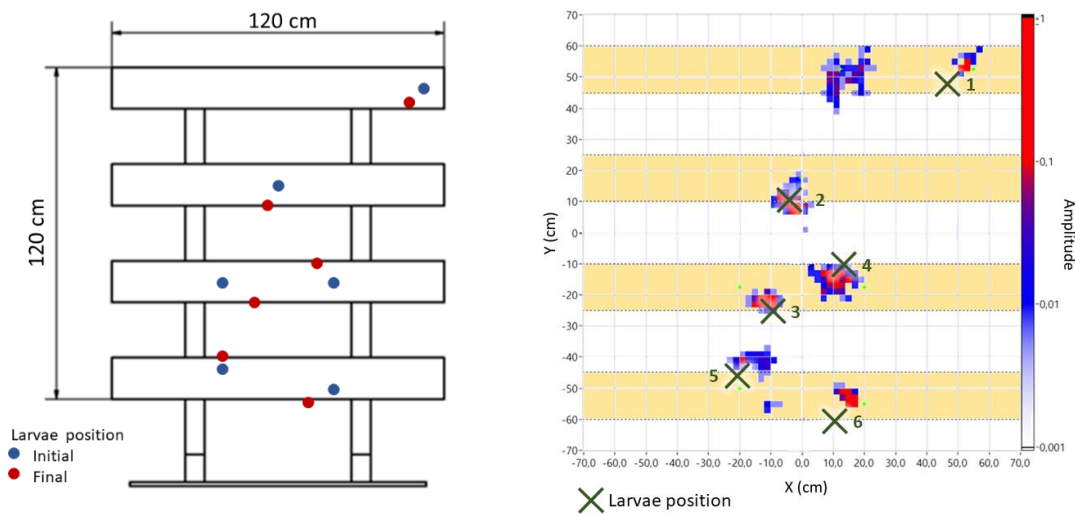
345 Figure 12. 2D histogram with estimated larvae positions from acoustic images.

346

347 **5.2 Verification of larvae trajectories inside the wooden beams**

348 All larvae survived implantation and during the 2-month period made tunnels from 110 mm to
 349 290 mm in length (Figure 13a). This shows that, despite the low moisture content of the wood,
 350 their activity was intense.

351 The wood anisotropy, differences in density between spring and summer wood, together with the
 352 presence of anomalies such as knots, cracks, etc. produce refraction and reflection phenomena so
 353 that the sound does not always radiate through the area of the wood face closest to the bite. This
 354 results in greater uncertainty in locating the larvae. Figure 13b shows the image generated by the
 355 array with the actual positions of each of the 6 larvae and the location obtained by the system,
 356 together with the level of energy received.



(a)

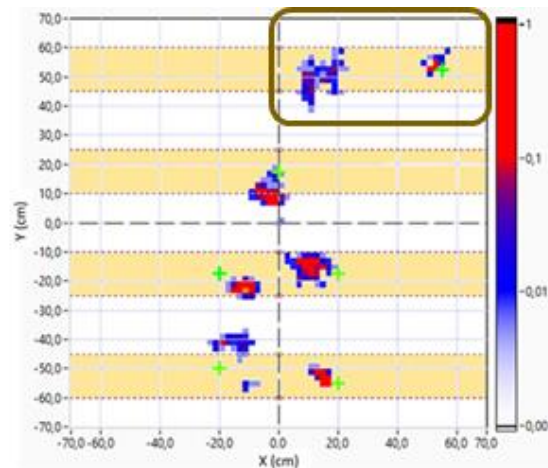
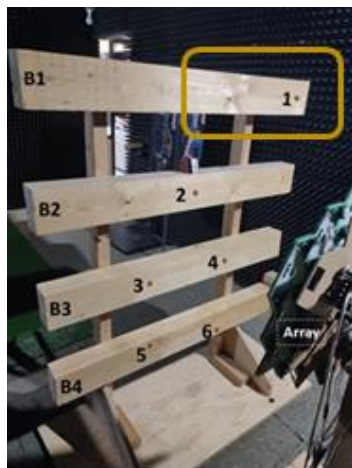
(b)

Figure 13. (a) Initial and final position of each of the larvae. (b) Location by the system and actual position of the larvae.

In the case of larva 1, it can be observed that there is a focus of sound emission to the left of the actual position of the larva. At this point, there is a fibre deflection due to a set of inclusive knots. This fibre deflection causes the growth rings being gnawed by the larva to surface. The speed of sound propagation is around 4 times higher, and the attenuation is lower in the fibre direction than in the perpendicular direction (Martinez et al. 2010). As can be observed in Figure 14, if the fibre bundle being eaten by the larva is lengthened, there is a deflection of fibres such that the fibres emerge at the surface close to a knot. This deflection of fibres acts as a conduit for better sound propagation. Next to larva 1 there is another more concentrated and more energetic detection focus that allows the larva to be located.

In the case of larvae 2 and 5, the device located the larvae in the air gap immediately below or above the wooden beams respectively. This is explained by the fact that the larvae were located on the side perpendicular to the observation face.

Larvae 3, 4 and 6 are correctly located by the equipment.



374

375 Figure 14. Simultaneous foci of sound emission from larva 1 due to fibre deflection.

376 O: origin of sound generated by larvae chewing, E: secondary output of sound.

377

378 **6. Conclusions**

379 A non-contact low-cost acoustic system, based on a low-cost MEMS microphone array, sensitive
380 to the acoustic signals produced by cerambycid larvae when they tear wood to feed, allowing the
381 detection and actual localisation of multiple individuals inside structural-sized pieces of wood,
382 has been developed.

383 The work indicates that different anomalies in the wood, mainly cracks and knots, can cause the
384 focus of the sound output and the place where the larva generates it to be distant. This results in
385 failures in larvae localization or a splitting of the localization. In any case, the error in the
386 localisation is inside the wood internode, which can be considered as the minimum unit of anti-
387 xylophagous treatment. Therefore, the system presented can be used to carry out specific
388 treatments as opposed to the extensive treatments currently used.

389 Bearing in mind that the growth of larvae is not linear, since the larger they are the more they can
390 grow, and that when they hatch they are so small that they cannot be heard, a future line of
391 research associated with this work could focus on the study of the influence of larva size on the
392 system's detection capacity, or on how larva size influences the detection threshold to be defined
393 for the system.

394 The study could also be extended to the detection of the feeding patterns **and the galleries of** other
395 xylophagous organisms, such as common woodworm or termites. Field tests could also be
396 conducted to evaluate their performance outside the laboratory environment. In the future, the
397 system could address the identification of the specific type of xylophage responsible for the
398 deterioration by using machine learning or equivalent techniques, based on the temporal and
399 frequency information of the detected sound events. This would allow for even more targeted and
400 localised curative treatments.

401

402 **Acknowledgments**

403 This research was funded by the Junta de Castilla y León, co-financed by the European Union
404 through the European Regional Development Fund (FEDER) (ref. VA228P20).

405

406 **Credit authorship contribution statement**

407 **Roberto D. Martínez:** Conceptualization, Methodology, Writing-original draft, Writing-review
408 and editing. **Alberto Izquierdo:** Conceptualization, Methodology, Investigation, Data curation,
409 Writing-original draft, **Juan José Villacorta:** Methodology, Investigation, Data curation. **Lara**
410 **del Val:** Investigation, Writing-original draft, Writing-review and editing. **Luis-Alfonso**
411 **Basterra:** Conceptualization, Writing-original draft, Writing-review and editing.

412 **Declaration of competing interest**

413 The authors declare that they have no known competing financial interests or personal
414 relationships that could have appeared to influence the work reported in this paper.

415

416 **References**

- 1 417 Beeby, S., G. Ensell, M. Kraft, and N. White. 2004. *MEMS Mechanical Sensors*. Edited by
2 418 Artech House Publishers. Norwood: Artech House Publishers.
- 3 419 Bilski, Piotr, Piotr Bobiński, Adam Krajewski, and Piotr Witomski. 2016. “Detection of Wood
4 420 Boring Insects’ Larvae Based on the Acoustic Signal Analysis and the Artificial
5 421 Intelligence Algorithm.” *Archives of Acoustics* 42 (1): 61–70.
6 422 <https://doi.org/10.1515/AOA-2017-0007>.
- 7
8 423 Brandstein, M.; Ward, D. *Microphone Arrays*; Springer: New York, NY, USA, 2001.
- 9
10 424 Cho Y.T.; Roan M.J., “Adaptive near-field beamforming techniques for sound source imaging”,
11 425 in *J Acoust Soc Am* 125, 944–957 (2009). <https://doi.org/10.1121/1.3050248>
- 12
13 426 Demelt, C. 1966. *Die Tierwelt Deutschlands, II. Bockkäfer Oder Cerambycidae. I Biologie*
14 427 *Mitteleuropäischer Bockkäfer Unter Besonder Berücksichtigung Der Larven*. Vol. II. Jena:
15 428 G. Fischer.
- 16
17 429 Dissanayake, Chinthaka M., Ramamohanarao Kotagiri, Malka N. Halgamuge, and Bill Moran.
18 430 2018a. “Improving Accuracy of Elephant Localization Using Sound Probes.” *Applied*
19 431 *Acoustics* 129 (January): 92–103. <https://doi.org/10.1016/j.apacoust.2017.07.007>.
- 20
21
22 432 ———. 2018b. “Improving Accuracy of Elephant Localization Using Sound Probes.” *Applied*
23 433 *Acoustics* 129 (January): 92–103. <https://doi.org/10.1016/j.apacoust.2017.07.007>.
- 24
25 434 Duffy, E.A.J. 1953. *A Monograph of the Immature Stages of British and Imported Timber*
26 435 *Beetles (Cerambycidae)*. London: British Museum (National History).
- 27
28 436 ———. 1957. *A Monograph of the Immature Stages of African Timber Beetles (Cerambycidae)*.
29 437 London: British Museum (National History).
- 30
31 438 Edstrand, A, C. Bahr, M. Williams, J. Meloy, T. Reagan, D. Wetzel, M. Sheplak, and L.
32 439 Cattafesta. 2011. “An Aeroacoustic Microelectromechanical Systems (MEMS) Phased
33 440 Microphone Array.” In *Proceedings of the 21st AIAA Aerodynamic Decelerator Systems*
34 441 *Technology Conference and Seminar*. Dublin.
- 35
36
37 442 Fujii, Y, M Noguchi, Y Imamura, and M Tokoro. 1989. “Detection of Termite Attack in Wood
38 443 Using Acoustic Emissions.” In *Proceedings IRG Annual Meeting*. Lappeenranta.
- 39
40 444 He T., Pan Q., Liu Y., Liu X., Hu D., “Near-field beamforming analysis for acoustic emission
41 445 source localization”, *Ultrasonics*, Volume 52, Issue 5, 2012, Pages 587-592,
42 446 <https://doi.org/10.1016/j.ultras.2011.12.003>.
- 43
44 447 Hsieh, C.T, J.-M. Ting, C. Yang, and C.K. Chung. 2002. “The Introduction of MEMS
45 448 Packaging Technology.” In *In Proceedings of the 4th International Symposium on*
46 449 *Electronic, Materials and Packaging*. Kaohsiung.
- 47
48
49 450 Kennedy R.A., Abhayapala T.D. and Ward D.B., "Broadband nearfield beamforming using a
50 451 radial beampattern transformation," in *IEEE Transactions on Signal Processing*, vol. 46,
51 452 no. 8, pp. 2147-2156, Aug. 1998, doi: 10.1109/78.705426.
- 52
53 453 Kershenbaum, Arik, Jessica L. Owens, and Sara Waller. 2019. “Tracking Cryptic Animals
54 454 Using Acoustic Multilateration: A System for Long-Range Wolf Detection.” *The Journal*
55 455 *of the Acoustical Society of America* 145 (3): 1619–28. <https://doi.org/10.1121/1.5092973>.
- 56
57 456 Mankin, R W, D W Hagstrum, M T Smith, A L Roda, and M T K Kairo. n.d. “Perspective and
58 457 Promise: A Century of Insect Acoustic Detection and Monitoring.” Accessed March 14,
59 458 2023. <https://academic.oup.com/ae/article/57/1/30/2462094>.
- 60
61
62
63
64
65

- 1 459 Mankin, R W, M T Smith, J M Tropp, E B Atkinson, and And D Y Jong. 2008. "Detection of
2 460 Anoplophora Glabripennis (Coleoptera: Cerambycidae) Larvae in Different Host Trees
3 461 and Tissues by Automated Analyses of Sound-Impulse Frequency and Temporal Patterns."
4 462 *J. Econ. Entomol* 101 (3): 838–49. <https://academic.oup.com/jee/article/101/3/838/806198>.
- 5 463 Mankin, R W, A Mizrach, A Hetzroni, S Levsky, Y Nakache, V Soroker. 2008. "Temporal and
6 464 Spectral features of sounds of Wood-Boring Beetle Larvae: identifiable patterns of
7 465 activity enable improved discrimination from background noise." *Florida Entomologist* 91
8 466 (2). [https://doi.org/10.1653/0015-4040\(2008\)91\[241:TASFOS\]2.0.CO;2](https://doi.org/10.1653/0015-4040(2008)91[241:TASFOS]2.0.CO;2).
- 9 467 Mankin, RW, DW Hagstrum, MT Smith, AL Roda, and MTK Kairo. 2011. "Perspective and
10 468 Promise: a Century of Insect Acoustic Detection and Monitoring." *American Entomologist*
11 469 57 (1). <https://doi.org/10.1093/ae/57.1.30>.
- 12 470 Mankin, Richard, David Hagstrum, Min Guo, Panagiotis Eliopoulos, and Anastasia Njoroge.
13 471 2021. "Automated Applications of Acoustics for Stored Product Insect Detection,
14 472 Monitoring, and Management." *Insects* 12 (3). <https://doi.org/10.3390/insects12030259>.
- 15 473 Martinez, Roberto, Ignacio Bobadilla, Guillermo Iñiguez, Francisco Arriaga, Miguel Esteban,
16 474 and Eva Hermoso. 2010. "Assessment of Decay in Existing Timber Members by Means of
17 475 Wave Velocity Perpendicular to the Grain." In *11th World Conference on Timber*
18 476 *Engineering 2010, WCTE 2010*, 1471–75. Riva di Garda.
- 19 477 Naidu, PS. *Sensor Array Signal Processing*, 1st ed; CRC Press: Boca Raton, FL, USA, 2001.
- 20 478 Noad, Michael J, Douglas H Cato, and M Dale Stokes. 2004. "ACOUSTIC TRACKING OF
21 479 HUMPBACK WHALES: MEASURING INTERACTIONS WITH THE ACOUSTIC
22 480 ENVIRONMENT." In *Proceedings of Acoustics*.
- 23 481 Nowakowska, Magdalena, Adam Krajewski, Piotr Witomski, and Piotr Bobiński. 2017.
24 482 "Thermic Limitation of AE Detection Method of Old House Borer Larvae (Hylotrupes
25 483 Bajulus L.) in Wooden Structures." *Construction and Building Materials* 136 (April):
26 484 446–49. <https://doi.org/10.1016/J.CONBUILDMAT.2017.01.012>.
- 27 485 Pallaske, M. 1986. "Measurement and Analysis of the Activity of Larvae of the House
28 486 Longhorn Beetle Hylotrupes Bajulus (L.) in Wood and in an Artificial Diet with the Aid of
29 487 Modern Electronics." *Material Und Organismen* 21 (1): 63–79.
- 30 488 Pence, Roy J, S J Magasin, and R G Nordberg. 1954. "Detecting Wood-Boring Insects
31 489 Electronic Device Developed as Aid in Locating Insects Destructive to Timber and Wood
32 490 Products."
- 33 491 Plinke, Burkhard. 2021. "InsectDetect Aktiver Schadinsekten Im Holzhandel."
34 492 <https://www.fnr.de/ftp/pdf/berichte/22WK412101.pdf>.
- 35 493 Potamitis, Ilyas, Iraklis Rigakis, Nicolaos-Alexandros Tatlas, and Stelios Potirakis. 2019. "In-
36 494 Vivo Vibroacoustic Surveillance of Trees in the Context of the IoT."
37 495 <https://doi.org/10.3390/s19061366>.
- 38 496 Ruiz, A. 1942. "Insectos Xilófagos: Cuatro Coleópteros de La Madera Labrada." *Boletín de*
39 497 *Patología Vegetal y Entomología Agrícola* 11: 201–39.
- 40 498 "SbRIO-9607 Platform." n.d. Accessed March 14, 2023. [https://www.ni.com/docs/en-](https://www.ni.com/docs/en-US/bundle/sbrio-9607-feature/page/overview.html)
41 499 [US/bundle/sbrio-9607-feature/page/overview.html](https://www.ni.com/docs/en-US/bundle/sbrio-9607-feature/page/overview.html).
- 42 500 "SPH0641LU4H-1 MEMS Microphone" n.d. Accessed March 18, 2023.
43 501 <https://www.knowles.com/docs/default-source/model-downloads/sph0641lu4h-1-revb.pdf>.

1
2
3
4
5
6
7
8
9
10
11
12
13
14
15
16
17
18
19
20
21
22
23
24
25
26
27
28
29
30
31
32
33
34
35
36
37
38
39
40
41
42
43
44
45
46
47
48
49
50
51
52
53
54
55
56
57
58
59
60
61
62
63
64
65

502 Sutin A, A Yakubovski, HR Salloum, TJ Flynn, N Sedunov, H Nadel. 2019. “Towards an
503 Automated Acoustic Detection Algorithm for Wood-Boring Beetle Larvae (Coleoptera:
504 Cerambycidae and Buprestidae)” *Journal of Economic Entomology* 112 (3).
505 <https://doi.org/10.1093/jee/toz016>

506 Tiete, Jelmer, Federico Domínguez, Bruno Da Silva, Laurent Segers, Kris Steenhaut, and
507 Abdellah Touhafi. 2014. “SoundCompass: A Distributed MEMS Microphone Array-Based
508 Sensor for Sound Source Localization.” *Sensors* 14. <https://doi.org/10.3390/s140201918>.

509 Trees, Harry L. Van. 2002. *Optimum Array Processing: Part IV of Detection, Estimation, and*
510 *Modulation*. Edited by John Wiley & Sons.
511 <https://books.google.es/books?id=J5TZDwAAQBAJ&dq=Van+Trees,+H.+Optimum+Arr>
512 [ay+Processing:+Part+IV+of+Detection,+Estimation+and+Modulation+Theory,+John+Wil](https://books.google.es/books?id=J5TZDwAAQBAJ&dq=Van+Trees,+H.+Optimum+Arr)
513 [ey+%26+Sons,+2002.++&lr=&hl=es&source=gbs_navlinks_s](https://books.google.es/books?id=J5TZDwAAQBAJ&dq=Van+Trees,+H.+Optimum+Arr).

514 Veen, Barry D. Van, and Kevin M. Buckley. 1988. “Beamforming: A Versatile Approach to
515 Spatial Filtering.” *IEEE ASSP Magazine* 5 (2): 4–24. <https://doi.org/10.1109/53.665>.

516 Vives, Eduard. 2000. *Fauna Ibérica, Coleóptera: Cerambycidae*. Vol. 12. Madrid: Museo
517 Nacional de Ciencias Naturales.

518 Zarco, E. 1935. “Sobre El Hallazgo En Santander de Un Coleóptero Perforador de Las
519 Cubiertas de Plomo de Cables Telefónicos.” *Boletín de La Real Sociedad Española de*
520 *Historia Natural* 35: 143–46.

521 Zhang, Xin, Enliang Song, Jingchang Huang, Huawei Liu, Yuepeng Wang, Baoqing Li, and
522 Xiaobing Yuan. 2014. “Acoustic Source Localization via Subspace Based Method Using
523 Small Aperture MEMS Arrays.” <https://doi.org/10.1155/2014/675726>.

524
525

Declaration of interests

The authors declare that they have no known competing financial interests or personal relationships that could have appeared to influence the work reported in this paper.

The authors declare the following financial interests/personal relationships which may be considered as potential competing interests:

Author statement

Roberto D. Martínez: Conceptualization, Methodology, Writing-original draft, Writing-review and editing. **Alberto Izquierdo:** Conceptualization, Methodology, Investigation, Data curation, Writing-original draft, **Juan José Villacorta:** Methodology, Investigation, Data curation. **Lara del Val:** Investigation, Writing-original draft, Writing-review and editing. **Luis-Alfonso Basterra:** Conceptualization, Writing-original draft, Writing-review and editing.